A Maxwell-Stefan-Glueckauf description of transient mixture uptake in microporous adsorbents

Krishna, R.

Link to publication

Citation for published version (APA):
Krishna, R. (2018). A Maxwell-Stefan-Glueckauf description of transient mixture uptake in microporous adsorbents. *Separation and Purification Technology, 191*, 392-399. https://doi.org/10.1016/j.seppur.2017.09.057

Separation and Purification Technology

Short Communication

A Maxwell-Stefan-Glueckauf description of transient mixture uptake in microporous adsorbents

Rajamani Krishna

Van 't Hoff Institute for Molecular Sciences, University of Amsterdam, Science Park 904, 1098 XH Amsterdam, The Netherlands

ARTICLE INFO

ABSTRACT

Based on the assumptions of uncoupled diffusion fluxes and loading-independent Fick diffusivities, the linear driving force (LDF) model developed by Glueckauf finds widespread usage in the modelling of transient mixture uptake in microporous adsorbents. A number of experimental investigations report overshoots in intra-crystal-line loadings of the more mobile species during transient binary mixture uptake in microporous adsorbents; these overshoots are not anticipated in the classic Glueckauf approach. The origins of the overshoots are traceable to strong coupling between species transfers engendered by mixture adsorption equilibrium thermodynamics; such coupling effects are most conveniently described by the Maxwell-Stefan (M-S) diffusion formulation. In this article, an explicit analytic model is developed to calculate transient mixture uptakes by combining the Maxwell-Stefan formulation with the linearization procedure of Glueckauf. The Maxwell-Stefan-Glueckauf model is validated by comparison with six different experimental data sets. In all six cases, the overshoots in the uptake of the more mobile partner species are properly captured; the incorporation of this approach in practical design procedures for adsorbers is expected to result in significant reduction in model complexity and computational times.

1. Introduction

Microporous adsorbents such as zeolites, carbon molecular sieves (CMS), metal-organic frameworks (MOFs), and zeolitic imidazolate framework (ZIFs) have potential applications in a wide variety of separation applications, that are commonly conducted in fixed bed devices. These devices are operated in a cyclical manner, with adsorption and desorption cycles [1–6]. The concentrations of the constituent species in the bulk fluid phase vary with position z along the bed, and time, t; see schematic in Fig. 1. At any position z in the fixed bed, and time t, the molar loadings in the adsorbed phase within the pores, varies along the radius of the particle, r. Most commonly, the separation performance in a fixed-bed adsorber is dictated by mixture adsorption equilibrium. Intra-particle diffusion

limitations cause distended breakthrough characteristics and usually lead to diminished separation effectiveness [2,3]. However, there are some instances of diffusion-selective operations in which diffusional effects over-ride the influence of mixture adsorption equilibrium and is the prime driver for separations [1,4,5,7]. Examples of diffusion-selective separations include: (1) selective uptake of N_2 from N_2/CH_4 mixtures using LTA-4A zeolite and Ba-ETS-4 [8–10], and (2) selective uptake of O_2 from O_2/N_2 mixtures using LTA-4A zeolite and CMS [5,11–14]. The development of such diffusion-selective processes requires accurate and robust models to describe transient mixture uptake within the adsorbent particles; the prime focus of this article is the development of such models. To set the scene, and define our objectives, we begin by examining the commonly used modelling approaches.

Nomenclature

b_i	Langmuir constant for species i, Pa^{-1}
$[B]$	matrix of inverse M-S coefficients, defined by Eq. (13), m^{-2} s
$Đ_i$	Maxwell-Stefan diffusivity for molecule-wall interaction, m^2 s^{-1}
$Đ_{ij}$	M-S exchange coefficient for n-component mixture, m^2 s^{-1}
$Đ_{12}$	M-S exchange coefficient for binary mixture, m^2 s^{-1}
$[D]$	matrix of Fick diffusivities, m^2 s^{-1}
f_i	partial fugacity of species i, Pa
n	number of species in the mixture, dimensionless
N_i	molar flux of species i with respect to framework, mol m^{-2} s^{-1}
p_i	partial pressure of species i in mixture, Pa
p_t	total system pressure, Pa
q_i	component molar loading of species i, mol kg^{-1}
$q_{i,sat}$	molar loading of species i at saturation, mol kg^{-1}
q_t	total molar loading in mixture, mol kg^{-1}
$\bar{q}_i(t)$	spatial-averaged component uptake of species i, mol kg^{-1}
$[Q]$	matrix defined in Eqs. (17) or (20), dimensionless

r	radial direction coordinate, m
r_c	radius of crystallite, m
R	gas constant, 8.314 J mol^{-1} K^{-1}
t	time, s
T	absolute temperature, K
x_i	mole fraction of species i in adsorbed phase, dimensionless
z	distance coordinate, m

Greek letters

Γ_{ij}	thermodynamic factors, dimensionless
$[\Gamma]$	matrix of thermodynamic factors, dimensionless
θ_i	fractional occupancy of component i, dimensionless
μ_i	molar chemical potential of component i, J mol^{-1}
ρ	framework density, kg m^{-3}

Subscripts

i	referring to component i
t	referring to total mixture
sat	referring to saturation conditions

The spatio-temporal distribution of molar loadings, q_i, within a spherical crystallite particle, of radius r_c, is obtained from a solution of a set of differential equations describing the transient uptake

$$\rho \frac{\partial q_i(r,t)}{\partial t} = -\frac{1}{r^2}\frac{\partial}{\partial r}(r^2 N_i); \quad i = 1,2\ldots n \tag{1}$$

The molar fluxes N_i are commonly related to the gradients in the molar loadings by Fick's law

$$N_i = -\rho D_i \frac{\partial q_i}{\partial r}; \quad i = 1,2\ldots n \tag{2}$$

An analytic solution to Eqs. (1) and (2) can be derived for the special case in which the following three constraints are satisfied: (1) the Fick diffusivity D_i for each of the components can be considered to be independent of the loading, (2) the initial locations at all locations r within the crystal are uniform, i.e. $q_i(r,0) = q_i(r_c,0)$, and (3) for all times $t \geq 0$, the exterior of the crystal is brought into contact with a bulk fluid mixture at partial fugacities $f_i(r_c,t)$ that is maintained constant till the crystal reaches thermodynamic equilibrium with the surrounding fluid mixture. The analytic solution, derived first by Geddes [15] to describe diffusion inside spherical vapor bubbles on distillation trays, is expressed as

$$\frac{(q_i^* - \bar{q}_i(t))}{(q_i^* - q_i(r_c,0))} = \frac{6}{\pi^2}\sum_{m=1}^{\infty}\frac{\exp\left(-m^2\pi^2\frac{D_i}{r_c^2}t\right)}{m^2} \tag{3}$$

where the spatial-averaged component loading at time t is

$$\bar{q}_i(t) = \frac{3}{r_c^3}\int_0^{r_c} q_i(r,t)r^2 dr \tag{4}$$

and q_i^* is the molar loading that is in equilibrium with the bulk fluid mixture.

In his classic paper, Glueckauf [16] derived the following simplified relation

$$\rho \frac{\partial \bar{q}_i(t)}{\partial t} = -\frac{15D_i}{r_c^2}(q_i^* - \bar{q}_i(t)); \quad i = 1,2\ldots n \tag{5}$$

that is valid for the condition $\frac{D_i t}{r_c^2} > 0.1$, along with the assumption $\frac{\partial \bar{q}_i(t)}{\partial t} \approx \frac{\partial q_i^*}{\partial t}$. The Glueckauf expression (5) is commonly referred to as the linear driving force (LDF) model. Sircar and Hufton [17,18] provide a fundamental rationalization for its widespread and successful use; they also take the view that the value of the constant need not be restricted to 15, and may be fitted match experiments.

The LDF model predicts that each component will approach equilibrium following

$$\frac{(q_i^* - \bar{q}_i(t))}{(q_i^* - q_i(r_c,0))} = \exp\left(-\frac{15D_i}{r_c^2}t\right); \quad i = 1,2\ldots n \tag{6}$$

Since the Fick diffusivities are assumed to be loading independent, Eq. (6) also implies that the approach to equilibrium for each species will be monotonous, i.e. without overshoots or undershoots.

Fig. 2 provides a compilation of experimental data on the transient spatially-averaged component loadings during transient uptake in four
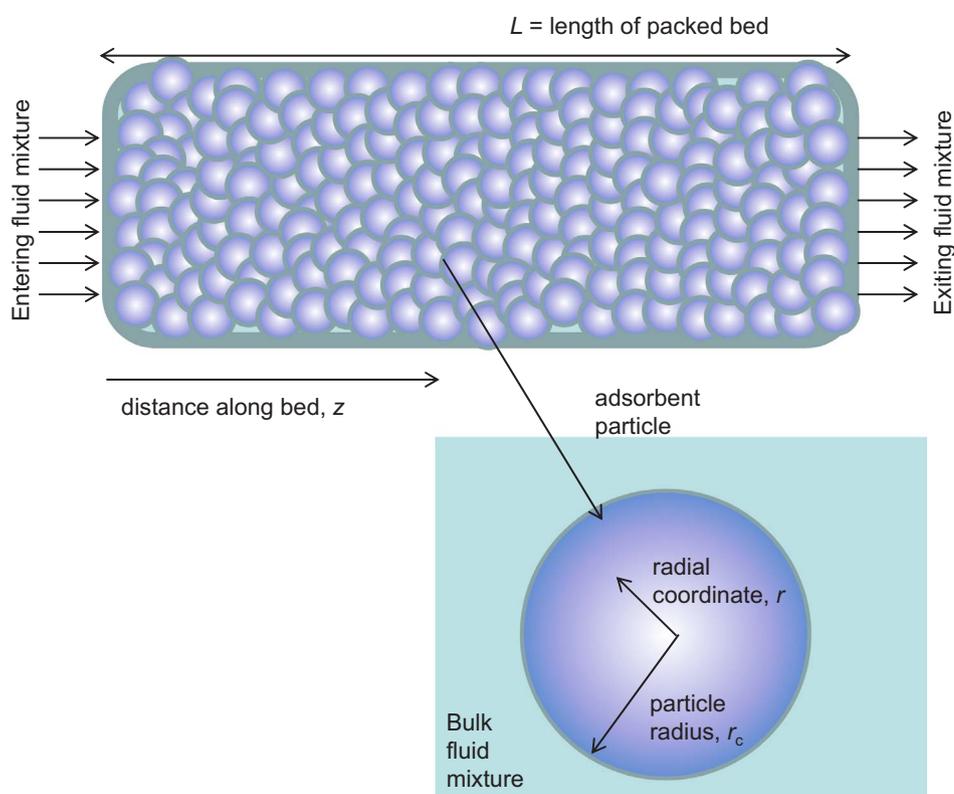
different host materials. In their experimental investigations using interference microscopy (IFM), Binder et al. [19] and Lauerer et al. [20] have monitored the uptake of CO_2, and C_2H_6 within crystals of DDR zeolite exposed to a bulk gas phase consisting of 1:1, 2:1, and 3:1 CO_2/C_2H_6 mixtures. In the three sets of experiments, overshoots in CO_2 loadings are observed during transient equilibration; see Fig. 2a–c. These experiments suggest the feasibility of devising a diffusion-selective process for selective adsorption of CO_2 from mixtures with ethane; see Fig. S5.

For transient uptake of N_2/CH_4 mixtures, overshoots in the loading of the more mobile N_2 have been reported for LTA-4A zeolite by Habgood [8]; see Fig. 2d. The experimental data of Saint-Remi et al. [21] for transient uptake of ethanol/1-propanol mixtures within SAPO-34, that is the structural analog of CHA zeolite, are shown in Fig. 2e; the more mobile ethanol is found to exhibit a pronounced maximum during the uptake transience. The experimental data of Titze et al. [22] for transient uptake of n-hexane(nC6)/2-methylpentane(2MP) mixtures in MFI zeolite crystal, exposed to an equimolar binary gas mixture at constant total pressure, shows a pronounced overshoot in the uptake of the more mobile linear isomer nC6; see Fig. 2f. In all the foregoing examples, the attainment of supra-equilibrium loadings signals uphill diffusion [23]. For all six data sets, the use of Eq. (6), shown by the
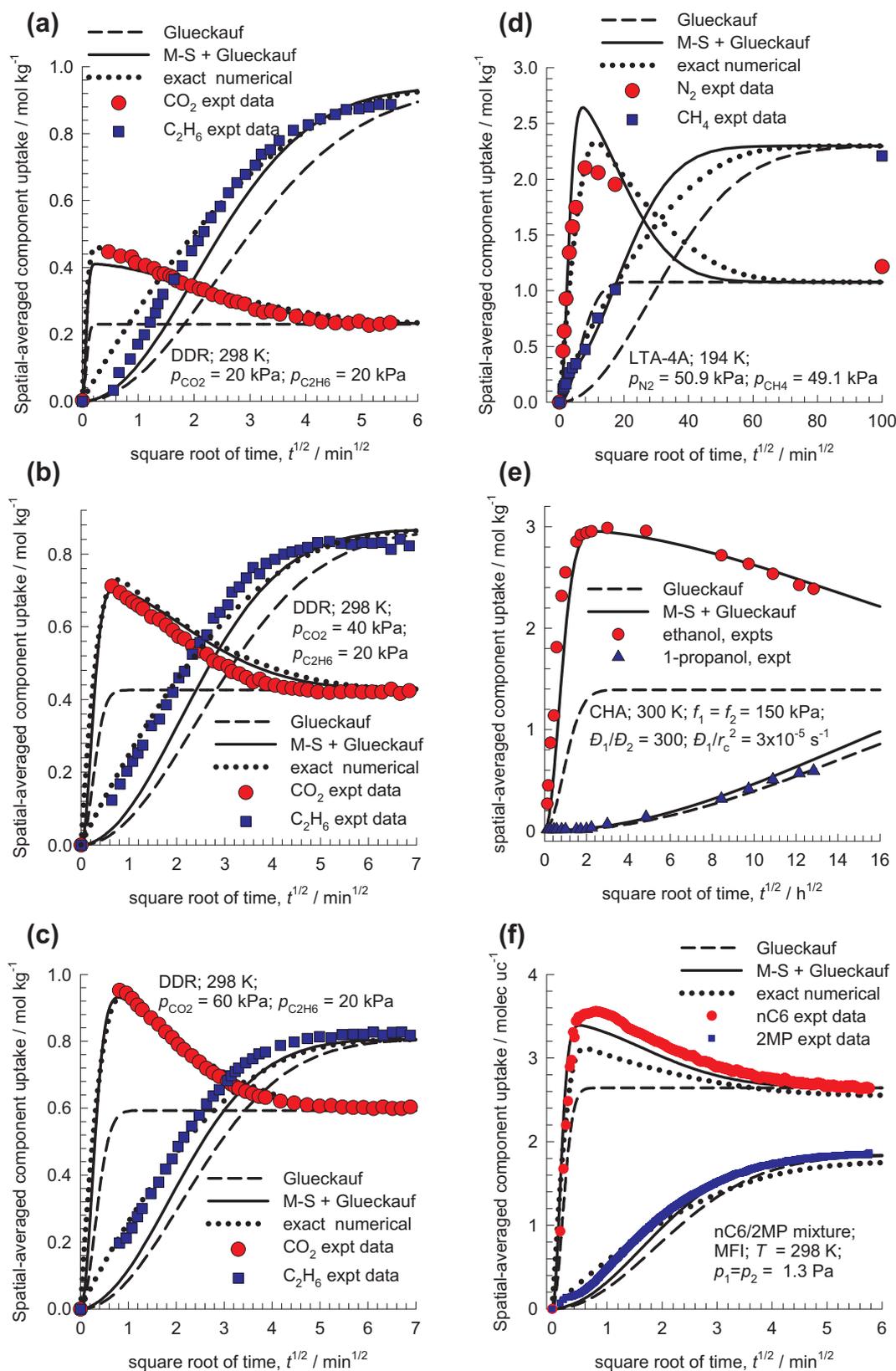
Fig. 2. (a–c) Experimental data of Binder et al. [19] and Lauerer et al. [20] (indicated by symbols) for spatial-averaged transient uptake of (a) 1:1 (b) 2:1, and (c) 3:1 $CO_2(1)/C_2H_6(2)$ gas mixtures within crystals of DDR zeolite at 298 K. (d) Experimental data of Habgood [8] on transient uptake of $N_2(1)/CH_4(2)$ mixture within LTA-4A crystals, exposed to binary gas mixtures at 194 K and partial pressures $p_1 = 50.9$ kPa; $p_2 = 49.1$ kPa. (e) Experimental data of Saint-Remi et al. [21] for transient uptake of ethanol/1-propanol mixtures within SAPO-34, that is the structural analog of CHA zeolite. (f) Experimental data (Run 1) of Titze et al. [22] for transient uptake of 50/50 nC6/2MP mixtures in MFI zeolite at 298 K and total pressure of 2.6 Pa. The dashed lines are the calculations using the classic Glueckauf model. The continuous solid lines are calculations based on the Maxwell-Stefan-Glueckauf model, developed in this work. The dotted lines are the calculations using the exact numerical solutions, as reported in the publication of Krishna [24]. All data inputs on isotherms and diffusivities are provided in the Supplementary material. Video animations 1–6 of the spatio-temporal development of component loadings have been uploaded as Supplementary material.

dashed lines, fails to capture the overshoots in the uptake of the more mobile partner species.

In a detailed analysis of these experimental data sets, Krishna [24] has demonstrated that the overshoots are caused by coupled species transfers, engendered by mixture adsorption thermodynamics. For quantitative modelling of transient uptakes it is necessary to adopt the Maxwell-Stefan (M-S) diffusion formulation in which the molar fluxes N_i are related to the gradients of the chemical potential:

$$-\rho \frac{q_i}{RT} \frac{\partial \mu_i}{\partial r} = \sum_{\substack{j=1 \\ j \neq i}}^{n} \left(\frac{x_j N_i - x_i N_j}{Đ_{ij}} \right) + \frac{N_i}{Đ_i}; \quad i = 1, 2, \ldots n \tag{7}$$

The x_i in Eq. (7) represent the component mole fractions in the adsorbed phase within the pores $x_i = q_i/q_t$; $q_t = \sum_{i=1}^{n} q_i$; $i = 1, 2, \ldots n$. The $Đ_i$ have the same significance as for unary diffusion; they are inverse drag coefficients between the species i and the pore walls; these diffusivities are determinable from unary uptake experiments.

The Onsager reciprocal relations demand the symmetry constraint

$$Đ_{ij} = Đ_{ji}; \quad i, j = 1, 2, \ldots n \tag{8}$$

The $Đ_{ij}$ may be interpreted as the inverse drag coefficient between species i and species j. At the molecular level, the $Đ_{ij}$ reflect how the facility for transport of species i *correlates* with that of species j; they are also termed *exchange coefficients*. The first members on the right hand side of Eq. (7) are required to quantify slowing-down effects that characterize binary mixture diffusion; slowing-down is caused because the jumps of the more mobile species are correlated with the jumps of the tardier partner species [25–27]. The exchange coefficients $Đ_{ij}$ cannot be determined directly from experiments. In some simple cases, use of Molecular Dynamics (MD) simulations [2,25–31] allow some insights to be gained on the characteristics of $Đ_{ij}$.

Generally, the set of Eqs. (1), (4) and (7) need to be solved numerically [24]; these are shown by the dotted lines in Fig. 2. The numerical solution is able to quantitatively capture the transient overshoots in all cases. Since the description of transient uptake within a single particle forms a subset of the overall model for a fixed bed adsorber (see Fig. 1), the implementation of the M-S formulation for intracrystalline diffusion is a challenging task, requiring the use of robust computational routines as detailed in earlier works [2,24]. The primary objective of this communication is to develop an explicit procedure to determine the transient uptake by developing analytic solutions to the M-S equations by a matrix generalization of the Glueckauf LDF approximation. Though the developed matrix relations are formally valid for *n*-component uptakes, the procedure is illustrated below for binary (*n* = 2) mixtures.

2. The Maxwell-Stefan-Glueckauf model development and results

For binary mixture diffusion, the Maxwell-Stefan Eq. (7) are written as

$$-\rho \frac{q_1}{RT} \frac{\partial \mu_1}{\partial r} = \frac{x_2 N_1 - x_1 N_2}{Đ_{12}} + \frac{N_1}{Đ_1}$$
$$-\rho \frac{q_2}{RT} \frac{\partial \mu_2}{\partial r} = \frac{x_1 N_2 - x_2 N_1}{Đ_{12}} + \frac{N_2}{Đ_2} \tag{9}$$

The gradients in the chemical potential can be related to the gradients of the molar loadings by defining thermodynamic correction factors Γ_{ij}

$$\frac{q_i}{RT} \frac{\partial \mu_i}{\partial r} = \sum_{j=1}^{n2} \Gamma_{ij} \frac{\partial q_j}{\partial r}; \quad \Gamma_{ij} = \frac{q_i}{f_i} \frac{\partial f_i}{\partial q_j}; \quad i, j = 1, 2 \tag{10}$$

where f_i are the partial fugacities in the bulk fluid mixture. The thermodynamic correction factors Γ_{ij} can be calculated by differentiation of
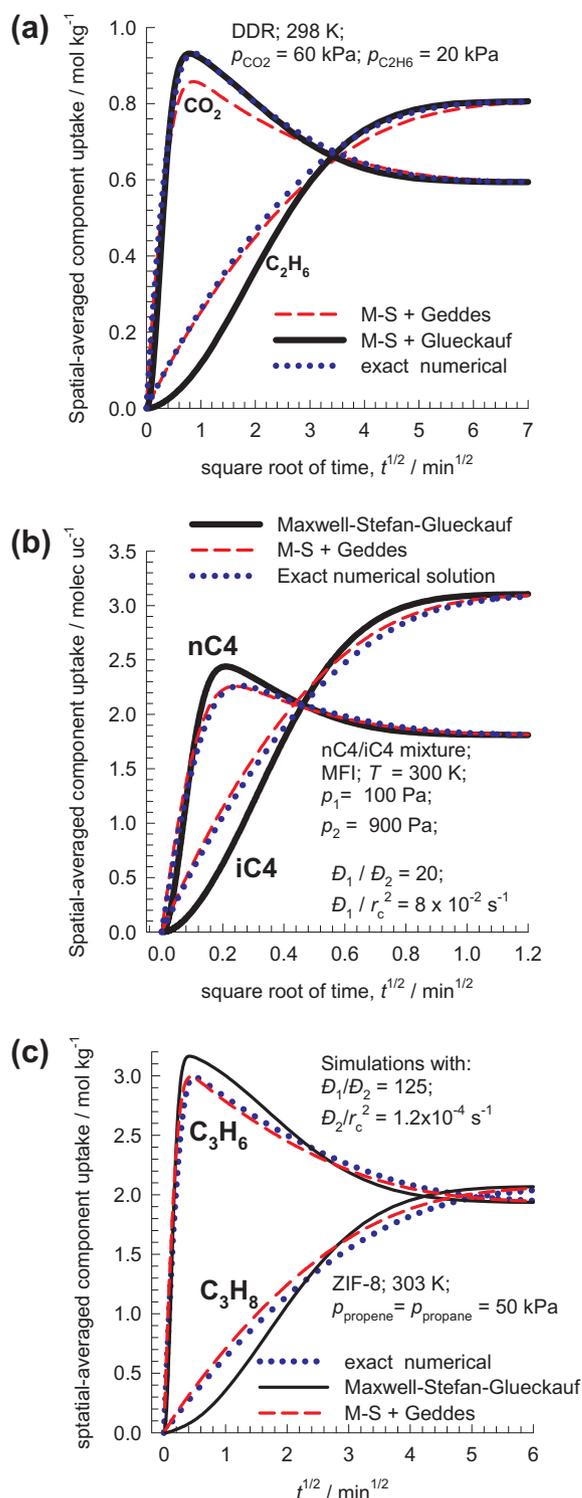

(a) DDR; 298 K; p_{CO2} = 60 kPa; p_{C2H6} = 20 kPa

CO₂

C₂H₆

- - - M-S + Geddes
—— M-S + Glueckauf
••••• exact numerical

(b) —— Maxwell-Stefan-Glueckauf
- - - M-S + Geddes
••••• Exact numerical solution

nC4

iC4

nC4/iC4 mixture; MFI; *T* = 300 K; p_1 = 100 Pa; p_2 = 900 Pa;

$Đ_1 / Đ_2$ = 20; $Đ_1 / r_c^2$ = 8 x 10^{-2} s⁻¹

(c) Simulations with: $Đ_1/Đ_2$ = 125; $Đ_2/r_c^2$ = 1.2x10^{-4} s⁻¹

C₃H₆

C₃H₈

ZIF-8; 303 K; $p_{propene}$ = $p_{propane}$ = 50 kPa

••••• exact numerical
—— Maxwell-Stefan-Glueckauf
- - - M-S + Geddes

Fig. 3. Comparison of three different models for calculations of transient uptake of (a) 3:1 CO_2(1)/C_2H_6(2) gas mixtures within crystals of DDR zeolite at 298 K, and (b) 1:9 n-butane(nC4)/i-butane(iC4) mixtures in MFI zeolite at 300 K, and (c) 1:1 C_3H_6/C_3H_8 mixtures in ZIF-8 at 303 K. The dashed lines are the calculations using the Maxwell-Stefan-Geddes model. The continuous solid lines are calculations based on the Maxwell-Stefan-Glueckauf model, developed in this work. The dotted lines are the calculations using the exact numerical solutions, as reported in the publication of Krishna [24].

the model describing mixture adsorption equilibrium. Generally speaking, the Ideal Adsorbed Solution Theory (IAST) of Myers and Prausnitz [32] is the preferred method for estimation of mixture adsorption equilibrium. In some special cases, the mixed-gas Langmuir model

$$\frac{q_1}{q_{1,sat}} = \theta_1 = \frac{b_1 p_1}{1 + b_1 p_1 + b_2 p_2}; \quad \frac{q_2}{q_{2,sat}} = \theta_2 = \frac{b_2 p_2}{1 + b_1 p_1 + b_2 p_2} \quad (11)$$

may be of adequate accuracy. For CO_2/C_2H_6 mixture adsorption in DDR zeolite, detailed comparison with IAST shows that the mixed-gas Langmuir model has been shown to be of good accuracy [24]. For the mixed-gas Langmuir model, Eq. (11), we can derive simple analytic expressions for the four elements of the matrix of thermodynamic factors [Γ]:

$$\begin{bmatrix} \Gamma_{11} & \Gamma_{12} \\ \Gamma_{21} & \Gamma_{22} \end{bmatrix} = \frac{1}{1-\theta_1-\theta_2} \begin{bmatrix} 1-\theta_2 & \frac{q_{1,sat}}{q_{2,sat}}\theta_1 \\ \frac{q_{2,sat}}{q_{1,sat}}\theta_2 & 1-\theta_1 \end{bmatrix} \quad (12)$$

where the fractional occupancies, θ_i, are defined by Eq. (11). The elements of the matrix of thermodynamic factors Γ_{ij} can be calculated explicitly from information on the component loadings q_i in the adsorbed phase; this is the persuasive advantage of the use of the mixed-gas Langmuir model. By contrast, the IAST does not allow the calculation of Γ_{ij} explicitly from knowledge on the component loadings q_i in the adsorbed phase; an implicit solution procedure is required. Even if the IAST is used to calculate the mixture adsorption equilibrium, the use of Eq. (12) to calculate the elements of the matrix of thermodynamic factors is a good approximation; evidence of this is provided by Krishna [24], for CO_2/C_2H_6 mixture adsorption in DDR zeolite.

For analysis of the systems in which the saturation capacities are different, the IAST has been consistently used in this work for calculation of mixture adsorption equilibrium for mixtures.

We define the square matrix [B] as

$$[B] = \begin{bmatrix} \frac{1}{Đ_1} + \frac{x_2}{Đ_{12}} & -\frac{x_1}{Đ_{12}} \\ -\frac{x_2}{Đ_{12}} & \frac{1}{Đ_2} + \frac{x_1}{Đ_{12}} \end{bmatrix} \quad (13)$$

A 2 × 2 dimensional Fick diffusivity matrix [D] is defined as the product of $[B]^{-1}$ and the matrix of thermodynamic correction factors [Γ]:

$$[D] = [B]^{-1}[\Gamma]$$

$$= \frac{1}{1 + \frac{x_1 Đ_2}{Đ_{12}} + \frac{x_2 Đ_1}{Đ_{12}}} \begin{bmatrix} Đ_1\left(1 + \frac{x_1 Đ_2}{Đ_{12}}\right) & \frac{x_1 Đ_1 Đ_2}{Đ_{12}} \\ \frac{x_2 Đ_1 Đ_2}{Đ_{12}} & Đ_2\left(1 + \frac{x_2 Đ_1}{Đ_{12}}\right) \end{bmatrix} \begin{bmatrix} \Gamma_{11} & \Gamma_{12} \\ \Gamma_{21} & \Gamma_{22} \end{bmatrix} \quad (14)$$

For unary diffusion, Eq. (14) degenerates to the familiar scalar equation $D = Đ\Gamma$. Correlation effects are of negligible importance for mixture diffusion in cage-type hosts such as LTA, DDR, CHA, ERI, and ZIF-8 that consist of cages separated by narrow windows in the 3.3–4.4 Å size range; the molecules hop one-at-a-time between cages [25–27,33]. In this scenario, $Đ_1 \ll Đ_{12}$; $Đ_2 \ll Đ_{12}$, and Eq. (14) simplifies to yield

$$[D] = \begin{bmatrix} Đ_1 & 0 \\ 0 & Đ_2 \end{bmatrix} \begin{bmatrix} \Gamma_{11} & \Gamma_{12} \\ \Gamma_{21} & \Gamma_{22} \end{bmatrix} \quad (15)$$

Combining Eqs. (9), (10), (13) and (14), we obtain the following explicit expression for the fluxes, expressed in 2-dimensional matrix notation as

$$(N) = -\rho[D]\frac{\partial(q)}{\partial r} \quad (16)$$

For the uptake of CO_2/C_2H_6 mixtures in DDR, N_2/CH_4 mixtures in LTA-4A, ethanol/1-propanol uptake in SAPO-34, Eq. (15) is the appropriate expression for the Fick diffusivity matrix [D]. By detailed consideration of correlation effects for nC6/2MP uptake in MFI zeolite, Titze et al. [22] have established the validity of Eq. (15) to model intra-crystalline fluxes. Since the matrix [Γ] is determined from mixture adsorption equilibrium, the modelling of all six data sets in Fig. 2 requires input data on just two parameters: $Đ_1/r_c^2$, and $Đ_2/r_c^2$; these input data are provided in the Supplementary Material.

The Fick diffusivity matrix [D] is a function of component loadings, and in the development of the linearized model, we determine the value of the [D] at the component loadings in equilibrium with the bulk fluid mixture, q_i^*; this diffusivity matrix is taken to be constant for the duration of the equilibration process. The matrix generalization of the Geddes Eq. (3) for constant [D] is discussed in detail in Chapter 9 of Taylor and Krishna [34]; the result is

$$(q^* - \bar{q}(t)) = [Q](q^* - q_0); \quad [Q] \equiv \frac{6}{\pi^2}\sum_{m=1}^{\infty}\frac{1}{m^2}\exp\left[-m^2\pi^2\frac{[D]t}{r_c^2}\right] \quad (17)$$

In Eq. (17), (q_0), (q^*), $(\bar{q}(t))$ represent, respectively, the 2-dimensional column matrices of component loadings corresponding to: initial conditions (zero for all the experiments shown in Fig. 2), at final equilibrium, and spatially-averaged values at time *t*. The Sylvester theorem, detailed in Appendix A of Taylor and Krishna [34], is required for explicit calculation of the 2 × 2 dimensional matrix [Q]. For the case of distinct eigenvalues, λ_1 and λ_2 of the Fick diffusivity matrix [D], the Sylvester theorem yields

$$[Q] = \frac{f(\lambda_1)[[D]-\lambda_2[I]]}{(\lambda_1-\lambda_2)} + \frac{f(\lambda_2)[[D]-\lambda_1[I]]}{(\lambda_2-\lambda_1)} \quad (18)$$

in which $f(\lambda_i) = \frac{6}{\pi^2}\sum_{m=1}^{\infty}\frac{1}{m^2}\exp\left[-m^2\pi^2\frac{\lambda_i t}{r_c^2}\right]$; $i = 1,2$.

If both the eigenvalues satisfy the condition $\frac{\lambda_i t}{r_c^2} > 0.1$, the matrix generalization of the Glueckauf expressions (5) and (6) are, respectively,

$$\rho\frac{\partial(\bar{q}(t))}{\partial t} = -\frac{15[D]}{r_c^2}(q^* - \bar{q}(t)) \quad (19)$$

and

$$(q^* - \bar{q}(t)) = [Q](q^* - q_0); \quad [Q] \equiv \exp\left[-\frac{15[D]t}{r_c^2}\right] \quad (20)$$

For evaluation of [Q] in Eq. (20), we apply Eq. (18), taking

$$f(\lambda_i) = \exp\left[-\frac{15\lambda_i t}{r_c^2}\right]; \quad i = 1,2.$$

As illustration, Fig. 3a presents a comparison of three different models for calculations of transient uptake of 3:1 $CO_2(1)/C_2H_6(2)$ gas mixtures within crystals of DDR zeolite at 298 K. The dotted lines are the calculations using the exact numerical solutions, as reported in the publication of Krishna [24]. The dashed lines are the calculations using the Geddes model, Eq. (17). We note that the analytic Geddes model is in reasonably good agreement with the exact numerical solution; this validates the matrix generalization procedure used to derive Eq. (17). The continuous solid lines are calculations based on Eq. (20), dubbed the Maxwell-Stefan-Glueckauf model; the obtained results for C_2H_6 loading is slightly less accurate than the exact numerical solution. Similar good agreement between the Maxwell-Stefan-Glueckauf model and exact numerical solutions is obtained for uptake of n-butane(nC4)/i-butane(iC4) in MFI zeolite (see Fig. 3b), C_3H_6/C_3H_8 in ZIF-8 (see Fig. 3c), O_2/N_2 in LTA-4A (see Fig. S12), and Kr/Xe uptake in SAPO-34 (see Fig. S16).

In Fig. 2, the continuous solid lines represent the calculations of the transient uptake using Eq. (20). In all six cases, the transient overshoots of the more mobile partner species are adequately captured, especially for the more mobile partner; the predictions for the tardier component is somewhat poorer because of slower equilibration. In comparison with the exact numerical solutions, presented in our earlier work [24], the agreement of the Maxwell-Stefan-Glueckauf model with experimental data is somewhat inferior. The linearization approximation used in deriving Eq. (20) may be of acceptable accuracy for implementation in process design of fixed bed adsorption devices.

3. Conclusions

The linear driving force (LDF) approximation developed by Glueckauf has been extended to include coupled diffusion effects by using the Maxwell-Stefan diffusion formulation. The key results of this work are Eqs. (19) and (20) that represent formal matrix generalizations of the commonly used Glueckauf formulations based on Fick's law. The implementation of the Maxwell-Stefan-Glueckauf model is straightforward, and involves only explicit numerical calculations requiring the use of Sylvester's formula (18). For the variety of cases examined, there is only a small sacrifice of computational accuracy in simulations of transient uptakes.

Another important message that emerges from this communication, is the necessity of including thermodynamic coupling effects, quantified by the matrix [Γ], in the calculation of the intra-crystalline transfer fluxes. The classic Glueckauf model essentially asserts that [Γ] equals the identity matrix; with this assumption, the transient overshoots of the more mobile species disappear. Interestingly, for the investigated guest/host combinations, transient permeation across membranes results in flux overshoots of the more mobile partners; see Figs. S4, S15, and S17.

Transient breakthrough simulations in fixed bed adsorbers carrying out diffusion-selective separations of CO_2/C_2H_6 mixtures with DDR zeolite (see Fig. S5), and N_2/CH_4 mixtures using LTA-4A zeolite (see Fig. S7) demonstrate that ignoring the influence of [Γ] leads to reduced productivities and separation capability.

Appendix A. Supplementary material

Supplementary data associated with this article can be found, in the online version, at http://dx.doi.org/10.1016/j.seppur.2017.09.057.

References

[1] D.M. Ruthven, S. Farooq, K.S. Knaebel, Pressure Swing Adsorption, VCH Publishers, New York, 1994.

[2] R. Krishna, The Maxwell-Stefan description of mixture diffusion in nanoporous crystalline materials, Microporous Mesoporous Mater. 185 (2014) 30–50.

[3] R. Krishna, Methodologies for evaluation of metal-organic frameworks in separation applications, RSC Adv. 5 (2015) 52269–52295.

[4] R.T. Yang, Gas Separation by Adsorption Processes, Butterworth, Boston, 1987.

[5] R.T. Yang, Adsorbents: Fundamentals and Applications, John Wiley & Sons Inc, Hoboken, New Jersey, 2003.

[6] R. Krishna, Screening metal-organic frameworks for mixture separations in fixed-bed adsorbers using a combined selectivity/capacity metric, RSC Adv. 7 (2017) 35724–35737.

[7] J. Kärger, D.M. Ruthven, D.N. Theodorou, Diffusion in Nanoporous Materials, Wiley-VCH, Weinheim, 2012.

[8] H.W. Habgood, The Kinetics of molecular sieve action. Sorption of nitrogen-methane mixtures by Linde molecular sieve 4A, Canad. J. Chem. 36 (1958) 1384–1397.

[9] S.J. Bhadra, S. Farooq, Separation of methane nitrogen mixture by pressure swing adsorption for natural gas upgrading, Ind. Eng. Chem. Res. 50 (2011) 14030–14045.

[10] B. Majumdar, S.J. Bhadra, R.P. Marathe, S. Farooq, Adsorption and diffusion of methane and nitrogen in barium exchanged ETS-4, Ind. Eng. Chem. Res. 50 (2011) 3021–3034.

[11] S. Farooq, M.N. Rathor, K. Hidajat, A predictive model for a kinetically controlled pressure swing adsorption separation process, Chem. Eng. Sci. 48 (1993) 4129–4141.

[12] S. Farooq, Sorption and diffusion of oxygen and nitrogen in molecular sieve RS-10, Gas Sep. Purif. 9 (1995) 205–212.

[13] Y.D. Chen, R.T. Yang, P. Uawithya, Diffusion of oxygen, nitrogen and their mixtures in carbon molecular-sieve, AIChE J. 40 (1994) 577–585.

[14] S. Sircar, A.L. Myers, Gas Separation by Zeolites, in: M. Auerbach, K.A. Carrado, P.K. Dutta (Eds.), Handbook of Zeolite Science and Technology, Marcel Dekker, New York, 2003, pp. 1063–1104 (Chapter 22).

[15] R.L. Geddes, Local efficiencies of bubble-plate fractionators, Trans. Am. Inst. Chem. Engrs. 42 (1946) 79–105.

[16] E. Glueckauf, Theory of chromatography. Part 10 – Formulae for diffusion into spheres and their application to chromatography, Trans. Faraday Soc. 51 (1955) 1540–1551.

[17] S. Sircar, J.R. Hufton, Why does the Linear Driving Force model for adsorption kinetics work? Adsorption 6 (2000) 137–147.

[18] S. Sircar, J.R. Hufton, Intraparticle adsorbate concentration profile for linear driving force model, AIChE J. 46 (2000) 659–660.

[19] T. Binder, A. Lauerer, C. Chmelik, J. Haase, J. Kärger, D.M. Ruthven, Micro-imaging of transient intracrystalline concentration profiles during two-component uptake of light hydrocarbon - carbon dioxide mixtures by DDR-type zeolites, Ind. Eng. Chem. Res. 54 (2015) 8997–9004.

[20] A. Lauerer, T. Binder, C. Chmelik, E. Miersemann, J. Haase, D.M. Ruthven, J. Kärger, Uphill diffusion and overshooting in the adsorption of binary mixtures in nanoporous solids, Nat. Commun. 6 (2015) 7697, http://dx.doi.org/10.1038/ncomms8697.

[21] J.C. Saint-Remi, G.V. Baron, J.F.M. Denayer, Non-uniform chain length dependent diffusion of short 1-alcohols in SAPO-34 in liquid phase, J. Phys. Chem. C 117 (2013) 9758–9765.

[22] T. Titze, C. Chmelik, J. Kärger, J.M. van Baten, R. Krishna, Uncommon synergy between adsorption and diffusion of hexane isomer mixtures in MFI zeolite induced by configurational entropy effects, J. Phys. Chem. C 118 (2014) 2660–2665.

[23] R. Krishna, Uphill Diffusion in multicomponent mixtures, Chem. Soc. Rev. 44 (2015) 2812–2836.

[24] R. Krishna, Tracing the origins of transient overshoots for binary mixture diffusion in microporous crystalline materials, Phys. Chem. Chem. Phys. 18 (2016) 15482–15495.

[25] R. Krishna, Describing the diffusion of guest molecules inside porous structures, J. Phys. Chem. C 113 (2009) 19756–19781.

[26] R. Krishna, Diffusion in porous crystalline materials, Chem. Soc. Rev. 41 (2012) 3099–3118.

[27] R. Krishna, J.M. van Baten, Investigating the influence of diffusional coupling on mixture permeation across porous membranes, J. Membr. Sci. 430 (2013) 113–128.

[28] R. Krishna, J.M. van Baten, Investigating the relative influences of molecular dimensions and binding energies on diffusivities of guest species inside nanoporous crystalline materials, J. Phys. Chem. C 116 (2012) 23556–23568.

[29] R. Krishna, J.M. van Baten, Influence of adsorption thermodynamics on guest diffusivities in nanoporous crystalline materials, Phys. Chem. Chem. Phys. 15 (2013) 7994–8016.

[30] R. Krishna, J.M. van Baten, Insights into diffusion of gases in zeolites gained from molecular dynamics simulations, Microporous Mesoporous Mater. 109 (2008) 91–108.

[31] R. Krishna, J.M. van Baten, Diffusion of alkane mixtures in MFI zeolite, Microporous

Mesoporous Mater. 107 (2008) 296–298.

[32] A.L. Myers, J.M. Prausnitz, Thermodynamics of mixed gas adsorption, AIChE J. 11 (1965) 121–130.

[33] R. Krishna, J.M. van Baten, A molecular dynamics investigation of the diffusion

characteristics of cavity-type zeolites with 8-ring windows, Microporous Mesoporous Mater. 137 (2011) 83–91.

[34] R. Taylor, R. Krishna, Multicomponent Mass Transfer, John Wiley, New York, 1993.